

Higher harmonic ECE spectrum and its change during ECRH in LHD

Shin KUBO, Hiroe IGAMI, Yoshio NAGAYAMA, Sadatsugu MUTO, Takashi SHIMOZUMA, Yasuo YOSHIMURA, Hiromi TAKAHASHI and Takashi Notake¹⁾

National Institute for Fusion Science, Toki 509-5292, Japan

¹⁾*FIR Center, University of Fukui, Fukui 910-8507, Japan*

(Received: 8 September 2008 / Accepted: 21 April 2009)

The calculation of the electron cyclotron emission (ECE) spectrum with the non thermal electron component is enabled solving the radiation transfer equation along the line of sight including the bi-Maxwellian distribution function. Such calculated ECE spectra are compared with the experimental ones during the high power electron cyclotron heated low density plasma where the high energy electrons in the range up to 100 keV are observed by the hard X-ray pulse height analysis. It is indicated that the ECE intensity lies in the thermal level due to the reabsorption at optically thick region, but becomes non-thermal from the relativistic down shifted emission at optically thin region. These results show that non-thermal ECE can be used to estimate the high energy electrons produced by the high power electron cyclotron heating.

Keywords: ECE, ECRH, supra-thermal electron, harmonic electron cyclotron spectrum

1. Introduction

Electron cyclotron emission (ECE) measurement has been established and widely used as a powerful diagnostic tool for the estimation of the local electron temperature, in particular with fast time response, in magnetic fusion experimental devices[1, 2]. Normally the electron temperature profile measurement by ECE relies on the local thermal equilibrium between radiation field and the electrons within black body condition. This black body condition can be qualitatively expressed by the optical thickness. Provided the plasma is optically thick and well in thermal equilibrium, the ECE spectra give electron temperature profile. It is also well known that ECE spectra are deformed by the presence of non-thermal electrons[3, 4] or in the case of optically thin or gray plasma[5]. In other words, this deformation of ECE spectra give the information of non thermal electrons and optical thickness that also depends on the non thermal electrons as well as bulk plasma parameters. The generation and the behavior of high energy electrons are especially important in high power electron cyclotron resonance heating (ECRH) in the helical plasma confinement magnetic configurations since they can play an essential role in controlling the electron flux that induces radial electric field in the collisionless regime.

The spectrum of electron cyclotron emission (ECE) is used to estimate the bulk electron temperature for optically thick plasma also in Large Helical Device (LHD)[6], but it is also sensitive to the supra-thermal electrons generated by high power ECRH, in particular at optically thin frequency region.

High power electron cyclotron resonance heating

(ECRH) is a powerful tool to control the local electron pressure and current, but heating and current drive themselves rely on the deformation of the electron velocity distribution function and can generate supra-thermal electrons. The generation of supra-thermal electrons can alter the power deposition profile by the change of absorption mechanism and the resultant supra-thermal electrons can drift out to broaden the power deposition profile by relaxing their energy at the other flux surfaces than the position where the power directly absorbed[7]. In order to clarify the generation mechanism of the supra-thermal electrons and their interaction with ECRH, second and higher harmonics ECE are calculated and compared with the experiment.

Experimental results on the supra-thermal electron generation on the low density LHD plasma by high power ECRH are described in section 2. The method of calculation and the results on the harmonic ECE emission spectra in LHD are described in section 3. These situations are estimated by extending existing ECE/ECRH absorption code and solving the radiation transfer equation using the Kirchhoff's radiation law[8, 9].

2. Experimental Results

High power ECRH experiments have been performed on relatively low density ($n_e \leq 0.3 \times 10^{19} \text{ m}^{-3}$) with total input power of 1.8 MW. Typical discharge waveforms are shown in Fig.1. ECRH power from one 77 GHz (from 9.5U port), one 84 GHz (from 1.5L port), two 82.7 GHz (from 5.5U and 9.5U ports) and three 168 GHz (from 5.5U and 2O ports) is injected in to LHD stepwise successively to attain 1.8

author's e-mail: kubo@LHD.nifs.ac.jp

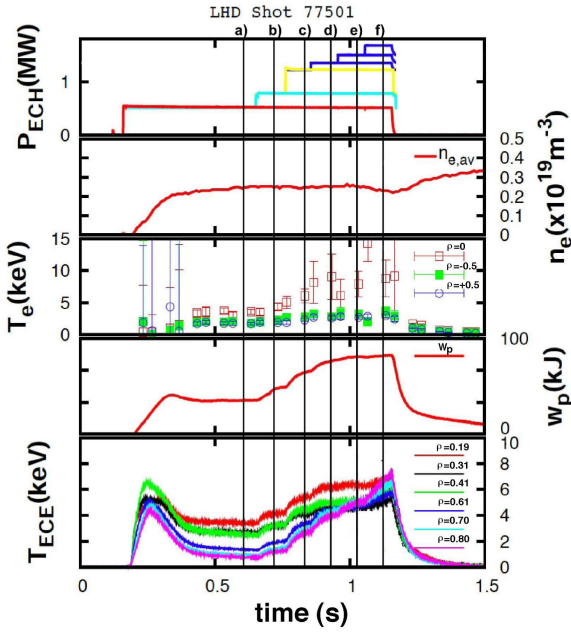


Fig. 1 Time evolutions of ECRH power P_{ECH} , averaged electron density n_e , Thomson temperature $T_e(\rho = 0, -0.5, +0.5)$, stored energy w_p and ECE radiation temperature $T_{ECE}(\rho = 0.19, 0.31, 0.41, 0.61, 0.70, 0.80)$, during low density, high power ECRH experiment.

MW in total [10]. Here, port label is the combination of a number that indicates toroidal number by helical pitch from a horizontally elongated cross section and U(upper), L (lower) O (outer) and I (inner). Therefore, U and L are preceded by a half integer, while O and I by an integer. Line of sight of ECE discussed here is along major radius in the horizontally elongated cross section (10I port) on the mid-plane of LHD from inner port. The density is adjusted to keep $n_e \leq 0.3 \times 10^{19} \text{ m}^{-3}$ as shown in the second column. Time evolution of the central and half radius electron temperature measured by Thomson scattering are plotted on the third column. Here the central electron temperature is plotted as the average of the of the 10 measuring points within ± 0.05 in normalized minor radius ρ . The central electron temperature increases as the power increased up to 1 MW, but the increase saturates or begins to scatter after the power exceeds 1MW. Stored energy increases almost in proportional to the injected ECRH power and finally reaches 80 kJ.

Electron temperature profiles at several power levels are shown in Fig.2. These profiles, especially at the last two time slices (Fig.2 e) and f)) show data scattering feature near the magnetic axis. In the bottom column of Fig.1 are shown the ECE radiation temperature evolutions at $\rho = 0.2, 0.3, 0.5, 0.6, 0.7,$

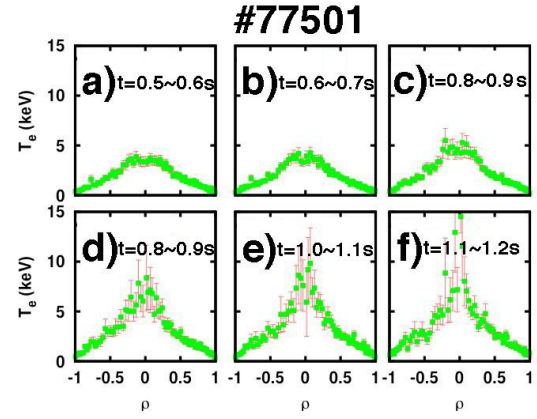


Fig. 2 T_e profiles at time slices indicated by arrows in Fig.1.

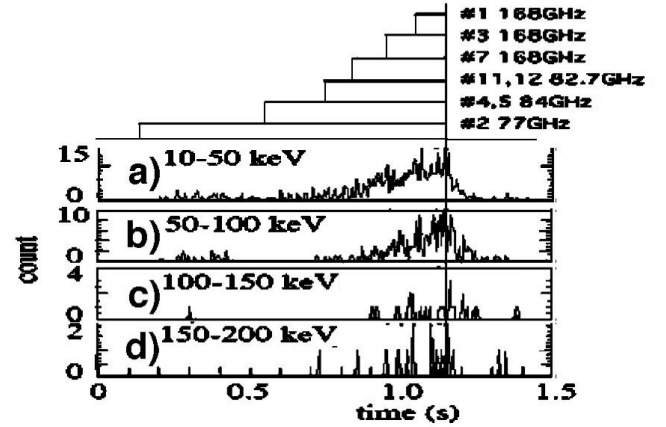


Fig. 3 Time evolution of the hard X-ray total intensity in a) less than 50 keV, b) 50-100 keV, c) 100-150 keV and d) 150-200 keV.

0.8. The peripheral ECE channels, corresponding to $\rho=0.7$ and 0.8 shown in the bottom column of Fig.1 clearly show non-thermal feature after 0.75 s when the ECRH injection power is more than 1 MW.

X-ray total emission intensity evolution in the energy range up to 200 keV and also Hard X-ray (HX) pulse height analysis (PHA) along several vertical chords are performed simultaneously. HX PHA chords are located in one of the vertically elongated cross sections of LHD (2.5L port), but apart from ECRH injection port (2O, 5.5U, 9.5U, and 1.5L). The X-rays at energy range of 10 to 100 keV increase as the injection power (and the temperature as a result) as shown in Fig.3 a) and b). Those at the energy range of more than 100 keV also begin to appear just in correspondence to the non-thermal feature of ECE discussed above, as shown in Fig.3 c) and d). These results suggest that high energy electrons of more than

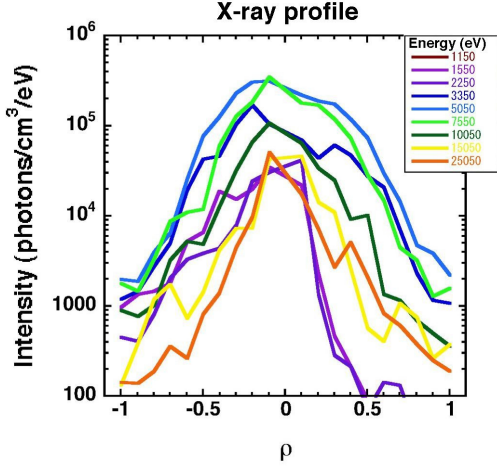


Fig. 4 Abel inverted intensity profile of X-ray intensity in the energy of 1-25 keV range.

100 keV are generated at high power of more than 1 MW ECRH phase. Abel inverted profile of the energy resolved X-ray intensity that the profile tends to be peaked as the energy increased but the peak positions are almost centered in every energy range as shown in Fig.4. These center peaked feature in any energy range in PHA suggest that the high energy electrons are populated near the center of the plasma.

In this experimental condition, the generation and collisional relaxation rate of electrons at 100 keV balance at the ECRH power level of 1 MW. Once the electrons reaches the critical energy, de-tuning effect limits the upper bound of energy gained by the ECRH, due to the relativistic down shift of the cyclotron frequency.

3. ECE spectrum calculation

In order to investigate the ECE spectrum with the presence of high energy components, calculation method integrating the radiation transfer equation in LHD is newly developed. The method is described in the first subsection and the results calculated with the typical parameters are shown in the second subsection.

3.1 Integration of the radiation transfer equation

The equation of radiation transfer can be given as:

$$\frac{dI(s)}{ds} = j_{\omega}(s) - \alpha_{\omega}(s)I(s), \quad (1)$$

here $I(s)$ is the radiation intensity at a given point s , $j_{\omega}(s)$ is the local emissivity and $\alpha_{\omega}(s)$ is the local absorption rate. The formal solution of this equation

can be given by

$$I(s) = \int \frac{j_{\omega}(s')}{\alpha_{\omega}(s')} e^{-\int_{s'}^s \alpha_{\omega}(s'') ds''} \alpha_{\omega}(s') ds', \quad (2)$$

assuming no background (multi-reflection) contamination. Kirchoff's radiation law relates the ratio of the emissivity to the absorption rate with the black body intensity as[8]:

$$B_0(s) = \frac{j_{\omega}(s)}{\alpha_{\omega}(s)}, \quad (3)$$

here, $B_0(s)$ is the black body intensity proportional to the local electron temperature $T_e(s)$ in case of single Maxwellian plasma and local radiation temperature, $T_{e,\text{rad}} \equiv \int f(\mathbf{v}) d\mathbf{v} / \int \frac{\partial f(\epsilon)}{\partial \epsilon} d\mathbf{v}$ for a general electron distribution function $f(\mathbf{v})$. A part of integrant of eq.(2) can be replaced by this local black body intensity and the radiation temperature can be expressed as an integration of local electron temperature as

$$T_{\text{rad},\omega} = \int T_e(s') e^{-\int_{s'}^s \alpha_{\omega}(s'') ds''} \alpha_{\omega}(s') ds' \quad (4)$$

in case of single Maxwellian plasma, and

$$T_{\text{rad},\omega} = \int T_{e,\text{rad}}(s') e^{-\int_{s'}^s \alpha_{\omega}(s'') ds''} \alpha_{\omega}(s') ds' \quad (5)$$

for a more general distribution function. Defining optical depth, $\tau_{\omega}(s)$ as

$$\tau_{\omega}(s) = \int_0^s \alpha_{\omega}(s') ds', \quad (6)$$

eq. (4) becomes well used formula:

$$T_{\text{rad},\omega} = \int T_e(s') e^{-\tau_{\omega}(s')} d\tau_{\omega}(s) \quad (7)$$

for a Maxwellian plasma, or

$$T_{\text{rad},\omega} = \int T_{e,\text{rad}}(s') e^{-\tau_{\omega}(s')} d\tau_{\omega}(s). \quad (8)$$

in case of arbitrary distribution function[9]. Equation (2) is valid even in the case where a multi-harmonics are included in the line of sight, by summing the absorption rate over multi harmonics as

$$\alpha_{\omega} = \sum_{i=1}^{\infty} \alpha_{\omega,i}, \quad (9)$$

here, $\alpha_{\omega,i}$ is the absorption rate at the i -th harmonic. The inclusion of higher harmonics is especially important in treating the high energy electrons due to the overlap of the relativistic down shift of the frequency. These integration along the line of sight of ECE measurement is performed taking the magnetic configuration and the profiles of plasma parameters into account. Actual calculation program is adopted from the ray-tracing code developed for ECRH in LHD [11]. The absorption rate of eq.(9) is calculated from weakly relativistic quasi-perpendicular formula appears in Ref.[12].

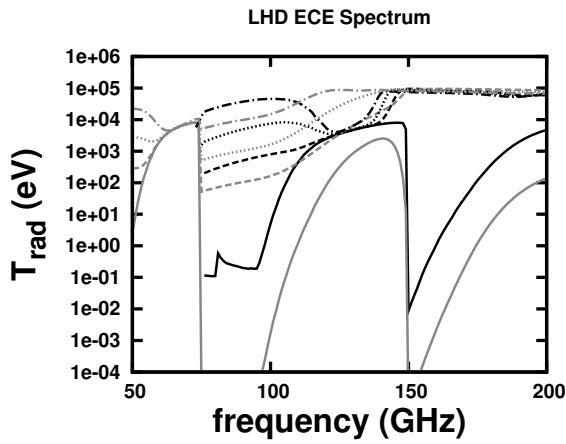


Fig. 5 Calculated spectra of ECE for a horizontal line of sight of LHD. All spectra are calculated for the bulk electron temperature at center of 8 keV with peaked profile and electron density at center of $5 \times 10^{18} \text{ m}^{-3}$ and flattened profile. Black and gray lines show those for X mode and O mode, respectively. Solid lines are those without high energy electrons. Broken, dotted and dash-dotted lines correspond to those with high energy density ratio of 0.01 %, 0.1 %, 1 % of bulk electrons, respectively. The energy of the included high energy electrons are fixed at 100 keV Maxwellian.

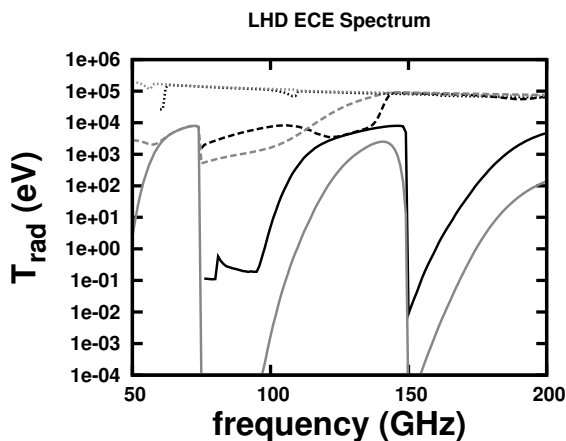


Fig. 6 Calculated spectra of ECE for an horizontal line of sight of LHD. All spectra are calculated for the bulk electron temperature at center of 8 keV with peaked profile and electron density at center of $5 \times 10^{18} \text{ m}^{-3}$ and flattened profile. Black and gray lines show those for X mode and O mode, respectively. Solid lines are those without high energy electrons. The spectra with high energy electrons of 100 keV and 1 MeV Maxwellian, are shown by broken and dotted lines respectively, keeping the density ratio of 0.1 %.

3.2 ECE spectrum calculation with non-thermal electrons

In the actual spectrum calculation, the effect of high energy electron is treated by defining bi-Maxwellian as the thermal electrons of Maxwellian

distribution function with experimentally observed electron temperature and density at each spatial point. High energy components are included by adding separate Maxwellian with assumed spatial profiles of density and temperature. Integration of the equation (5) or (8) is performed back along the line of sight.

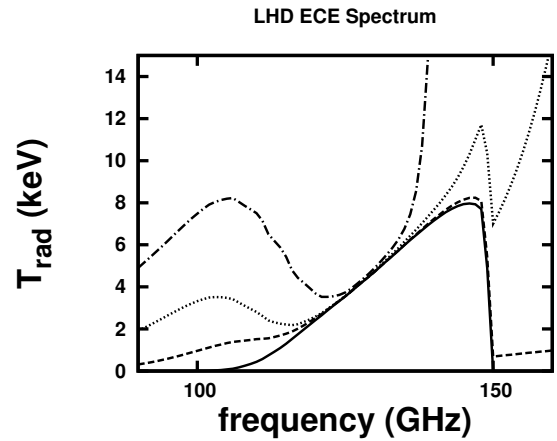


Fig. 7 Detail of the calculated spectra of X mode ECE for a horizontal line of sight of LHD of Fig.6 without (solid line) and with 50 keV (broken line), 75 keV (dotted line) and 100 keV (dash-dotted line) high energy component. The density ratio of high energy component to the bulk is fixed at 0.1 %.

In Fig.5 are shown the calculated spectra for X and O mode without and with the high energy electrons of 100 keV of 0.01 %, 0.1% and 1% bulk density. The energy and the density profiles are assumed to be the same as the bulk electrons. The shape of the spectrum without high energy component reflects the bulk electron temperature profile and the change of the magnetic field strength along the line of sight. The spectrum gap near 80 and 160 GHz is the gap between the fundamental and the second, the second and the third harmonic emission. When the high energy component is included, the gap between the second and the third harmonic emission is completely filled by the pile up of relativistic down shifted higher harmonic emissions even with the density ratio of 0.01%. The emission of the frequency corresponding to the second harmonic at the core plasma region (120 to 130 GHz) is strongly absorbed due to the high optical thickness and becomes almost thermal level.

In Fig.6 are shown the calculated spectra for X and O mode without and with the high energy electrons of 100 keV, 1MeV. Here, the density of the high energy component is fixed at 0.1 %. The energy and the density profile are assumed to be the same as the bulk electrons also in these cases. When the high energy component is included, the spectrum gaps tend to be filled by the relativistic down shifted higher har-

monic emission. Spectra at higher harmonics of more than 3rd show with high energy components become flat. Even with non-thermal emission due to the presence of high energy electrons, re-absorption occurs at optically thick region and mode, those corresponds to the core region of fundamental O mode and second harmonic X mode at the high energy components of below 100 keV. Spectra at optically gray region become non-thermal. Relativistically down shifted emission always experience the re-absorption since the observation antenna of ECE is normally in the low field side. These results indicate that ECE spectra are sensitive to the presence of high energy electrons only at lower frequency, optically thin region.

In order to compare and estimate the energy range and density ratio of high energy electrons produced by applying ECRH, X mode of Fig.6 is replotted as linear scale and depicting only the second harmonic region, and adding 50 keV and 75 keV cases in Fig.7. Here, high energy electrons are assumed to have 50, 75 and 100 keV with the density ratio of 0.1%. Suggested energy range is between 75 to 100 keV from the comparison between the bottom of Fig.1 and 7.

4. Summary

High energy electrons are created by high power, low density ECRH plasma. X-ray measurements show that more than 100 keV electrons are created and these electrons are localized near the magnetic axis. Appearance of non-thermal emission at frequencies corresponding to the 2-nd harmonics of peripheral region coincide with the high energy electrons.

The method of ECE spectrum calculation solving radiation transfer equation along the line of sight are described. The change in ECE spectrum due to the presence of high energy electrons at optically thick frequency is small due to re-absorption. The change in ECE spectra is more sensitive at optically gray or thin frequency which corresponds to the 2nd harmonic electron cyclotron at plasma peripheral region.

These results indicated that the ECE spectra are sensitive to the presence of high energy electrons, but re-absorption mechanism suppress the non-thermal emission at optically thick region. The possibility of deducing the high energy electron component from ECE measurement is indicated. Measured and calculated ECE spectra show in good correspondence assuming the high energy electron of 75 to 100 keV and 0.01-0.1 % of bulk electron density. Detailed comparison of the measured and calculated ECE spectra is left for the future work.

- [1] F. Engelmann and M. Curatolo, Nucl. Fusion **13** (1973) 497.
- [2] H. J. Harffuss, Plasma Phys. and Controlled Fusion **40** (1998) A231.
- [3] M. Tamor, Nuclear Fusion **18** (1978) 229.

- [4] G. Taylor *et al.*, Plasma Phys. and Controlled Fusion **31** (1989) 1957.
- [5] H. Idei *et al.*, Jpn. J. Appl. Phys. **33** (1994) 1543.
- [6] Y. Nagayama *et al.*, J. Plasma Fusion Res. **79** (2003) 601.
- [7] S. Kubo *et al.*, J. Plasma Fusion Res. SERIES **5** (2002) 584.
- [8] G. Bekefi, *Radiation Processes in Plasma*, John Wiley & Sons Inc., New York (1966).
- [9] N. Marushchenko *et al.*, Plasma and Fusion Research, **2** (2007) S1129.
- [10] S. Kubo, *et al.*, Plasma Physics and Controlled Fusion, **47** (2005) A81 .
- [11] S. Kubo *et al.*, Proc. 11th ICPP (2002)133.
- [12] M. Bornatici *et al.*, Nuclear Fusion **23** (1984)1153.